

# Large-scale power in the CMB and new physics: An analysis using Bayesian model comparison

Anastasia Niarchou, Andrew H. Jaffe, and Levon Pogosian  
 Blackett Laboratory, Imperial College London, SW7 2AZ, United Kingdom  
 (Received 26 August 2003; published 24 March 2004)

One of the most tantalizing results from the Wilkinson Microwave Anisotropy Probe (WMAP) experiment is the suggestion that the power at large scales is anomalously low when compared to the prediction of the “standard”  $\Lambda$  cold dark matter (CDM) model. The same anomaly, although with somewhat larger uncertainty, was also previously noted in the COBE data. In this work we discuss possible alternate models that give better fits on large scales and apply a model-comparison technique to select amongst them. We find that models with a cutoff in the power spectrum at large scales are indeed preferred by data, but only by a factor of 3.6, at most, in the likelihood ratio, corresponding to about “ $1.6\sigma$ ” if interpreted in the traditional manner. Using the same technique, we have also examined the possibility of a systematic error in the measurement or prediction of the large-scale power. Ignoring other evidence that the large-scale modes are properly measured and predicted, we find this possibility somewhat more likely, with roughly a  $2.75\sigma$  evidence.

DOI: 10.1103/PhysRevD.69.063515

PACS number(s): 98.80.Cq

## I. INTRODUCTION

The recent Wilkinson Microwave Anisotropy Probe (WMAP) results [1] have provided a spectacular view of the early Universe. One of the most intriguing results offered by the WMAP team is that the cosmic microwave background (CMB) anisotropy power on the largest angular scales seems to be anomalously low [1,2]. In fact, the WMAP team reports that this result has a high statistical significance, quoting a probability ranging from just under 1% to  $2 \times 10^{-3}$  for such a result, depending on the details of the analysis. This low power can be seen in two complementary ways. First, in the CMB power spectrum,  $C_\ell$ , the quadrupole ( $\ell=2$ ) and octopole ( $\ell=3$ ) both seem low in comparison to the smooth “best-fit” model, as shown in Fig. 1. The latter is selected from the array of models with a flat geometry and nearly-scale-invariant, adiabatic primordial fluctuations.

The low power seems particularly striking when the CMB anisotropy correlation function,

$$C(\theta) \equiv \langle T(\hat{\mathbf{n}})T(\hat{\mathbf{m}}) \rangle \quad \text{with} \quad \hat{\mathbf{n}} \cdot \hat{\mathbf{m}} = \cos \theta \quad (1)$$

is examined: it is very near zero for  $\theta \gtrsim 60^\circ$ . Note that the average implied by the angle brackets has several different, inequivalent, interpretations: The WMAP team estimates the correlation function calculated as the simple average over pixels at a given separation. If we interpret the average as an ensemble average, however, we can relate the correlation function to the power spectrum,  $C_\ell$ :

$$C(\theta) = \sum_{\ell} \frac{2\ell+1}{4\pi} C_\ell P_\ell(\cos \theta). \quad (2)$$

For a Gaussian distribution with enough samples, these two definitions are nearly equivalent, since the pixel average will approximate the ensemble average. We were able to reproduce the character of the correlation function from the published angular power spectrum, by summing the Legendre series in Eq. (2). In fact, we obtained almost the same result by using the smooth best-fit spectrum, but with the quadru-

pole and octopole lowered to the observed levels, as also shown in Fig. 2. (In fact, the correlation function in this case is actually flatter at  $\theta \sim 180^\circ$  than those computed from the actual data: the power in any of the correlation functions calculated from real data shows a lower correlation amplitude than those calculated from smooth power spectra.) Conversely, raising the quadrupole and octopole in the observed spectrum to the predicted levels removes the anomaly. This exercise implies that the low power is just that: low power at low  $\ell$ , and due neither to a conspiracy of particular  $C_\ell$  values nor to any non-Gaussian distribution of the multipole moments themselves. Moreover, the apparently striking difference between the measured and predicted  $C(\theta)$  is due entirely to the low values of the quadrupole and octopole. In this paper, we investigate the statistical significance of these measurements.

In the following, we introduce the Bayesian model-comparison method in Sec. II, discuss models with low primordial power in Sec. III, and a model of experimental or

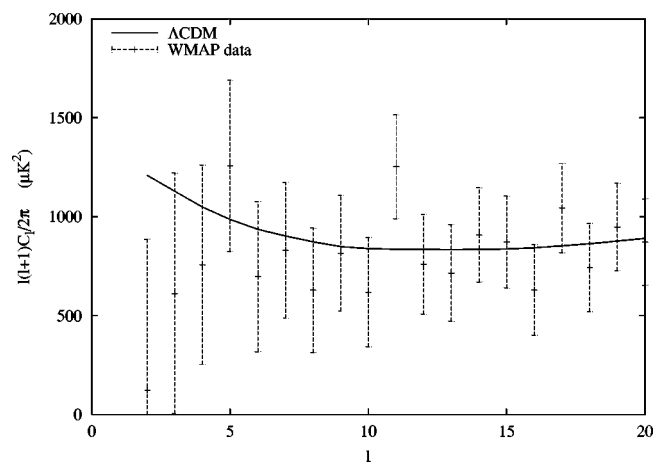


FIG. 1. The CMB power spectrum at low  $\ell$  as measured by WMAP. The solid line is the best fit using the “standard” power-law  $\Lambda$ CDM model. Note that the error bars at low multipoles are almost entirely due to cosmic variance.

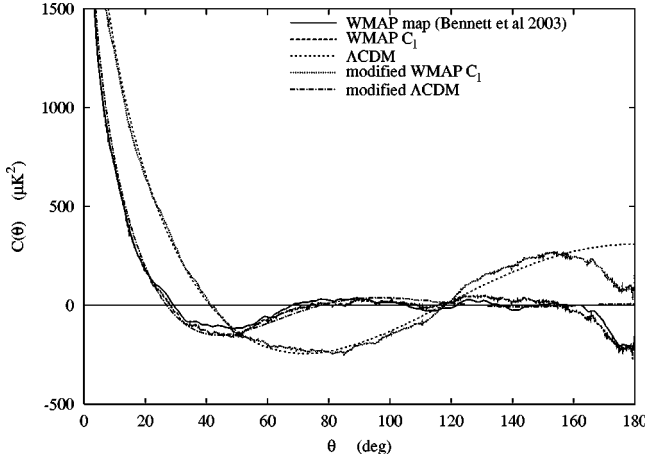


FIG. 2. The correlation function  $C(\theta)$  as computed from the WMAP team, from the pixelized map (solid line); using the  $C_\ell$ 's measured by WMAP (long dashed line), using WMAP's best fit  $C_\ell$  (short dashed), using the WMAP data with  $C_2$  and  $C_3$  changed to equal those of the best fit (dotted), and using the best-fit  $C_\ell$ 's with lowered values of  $C_2$  and  $C_3$  (dot-dash).

theoretical systematic errors in Sec. IV. We conclude with a discussion in Sec. V.

## II. MODEL COMPARISON

The question remains, then: How significant is this observed low power? Here, we shall answer this question using the technique of Bayesian model comparison [3,4]. This technique has been used before in various cosmological contexts [5–8].

We start, as usual, with Bayes' theorem, which gives the posterior probability of some theoretical parameters  $\theta$  given data  $D$  under the hypothesis of some model  $m$ :

$$P(\theta|DI_m) = P(\theta|I_m) \frac{P(D|\theta I_m)}{P(D|I_m)}, \quad (3)$$

where  $P(A|B)$  gives the probability or probability density of a proposition  $A$  given a proposition  $B$ , and here *all* probabilities are conditional, at least on the background information  $I_m$ , which refers to the background information for a specific model  $m$ . The model parameters  $\theta$  (the list of which may actually depend on which model  $m$  we consider) have prior probability  $P(\theta|I_m)$ . The likelihood function is  $P(D|\theta I_m)$ , and the so-called “evidence” is

$$P(D|I_m) = \int d\theta P(\theta|I_m) P(D|\theta I_m), \quad (4)$$

which enforces the normalization condition for the posterior but is also quite properly the probability of the data given model  $m$ , the “model likelihood.”

We can further factor the evidence as

$$P(D|I_m) = \mathcal{L}_m(\theta_{\max}) O_m, \quad (5)$$

where  $\theta_{\max}$  are the parameters that maximize the likelihood for model  $m$ ,  $\mathcal{L}_m(\theta) = P(D|\theta I_m)$ , and  $O_m$  is the so-called

“Ockham factor” [3]. The Ockham factor is essentially the ratio of the prior probability volume to the posterior probability volume. (This is most easily seen for the case where both prior and posterior are uniform distributions. When both are Gaussian distributions, the Ockham factor is the ratio of the determinants of the covariance matrices, which is indeed the ratio of the  $1\sigma$  volumes.)

In order to select among models, one usually employs the ratio of their probabilities:

$$\frac{P(m|DI)}{P(n|DI)} = \frac{P(m|I)}{P(n|I)} \frac{P(D|I_m)}{P(D|I_n)} = \frac{P(m|I)}{P(n|I)} B_{mn}. \quad (6)$$

Any experimental information is contained in the ratio of the evidence,  $B_{mn}$ , which is referred to as the “Bayes factor.” Lacking any prior information preferring one model over the other, Eq. (6) only depends on the Bayes factor. Equations (4)–(6) imply that the Bayes factor incorporates the essence of the Ockham razor: since the evidence is an average of the likelihood function with respect to the prior on the parameters, simpler models having a more compact parameter space are favored, unless more complicated models fit the data significantly better. Bayes factors are likelihood ratios and can be interpreted roughly as follows, as suggested in Ref. [9]: If  $1 < B_{mn} \leq 3$ , there is evidence in favor of model  $m$  when compared with  $n$ , but it is almost insignificant. If  $3 \leq B_{mn} \leq 20$ , the evidence for  $m$  is definite, but not strong. Finally, if  $20 \leq B_{mn} \leq 150$ , this evidence is strong and for  $B_{mn} \geq 150$  it is very strong.

We can also interpret the likelihood ratio in the same manner as we compute the “number of sigma” by which a value or hypothesis is favored. In this case the model is favored by  $\nu \sigma$  with  $\nu = \sqrt{2 \ln |B_{mn}|}$ . Another useful interpretation, perhaps more familiar to the engineering community, would be to use decibels,  $0.1 \log_{10} B_{mn}$  [3].

The model-comparison formalism outlined here *requires* us to specify alternatives to the “fiducial” standard model. Thus a sharper version of our question might be: Is it more probable that the data do reflect a standard Big Bang, with nearly-scale-invariant, adiabatic, isotropic, Gaussian fluctuations, or do they come from a universe with, say, a cutoff in the power spectrum? Or could there be a problem in the data analysis so that, say, the error bars are larger than thought, or the reported results somehow exhibit an oversubtraction of large-scale power? In the following we shall examine these possibilities.

The “fiducial” standard model is the best-fit model from Ref. [2]. It is a flat  $\Lambda$ CDM Friedmann-Robertson-Walker (FRW) universe, with baryon density  $\Omega_b = 0.046$  and “dark energy” density  $\Omega_\Lambda = 0.73$  (in units of the FRW critical density). It has a power-law initial matter power spectrum with spectral index  $n_s = 0.99$  and a present-day expansion rate of  $H_0 = 100h \text{ km sec}^{-1} \text{ Mpc}^{-1}$  with  $h = 0.72$ . The power spectrum amplitude is  $A_s = 0.855$ , as defined in the CMBFAST program [10] and as used by the WMAP team [11], related to the amplitude of fluctuations at  $k_0 = 0.05 \text{ Mpc}^{-1}$ .

The evidence for this model is simply the likelihood  $P(D|\theta_{\text{fiducial}})$  evaluated at the best-fit values of the parameters. We calculate the likelihood using the code provided by

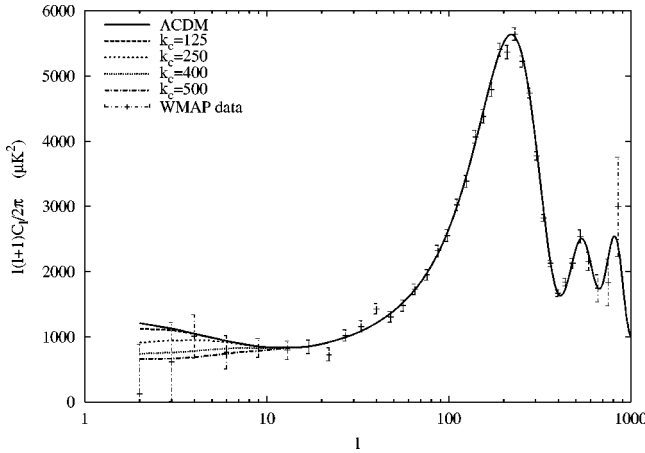


FIG. 3. CMB power spectra for various values of the cutoff parameter  $k_c$  of Eq. (7), measured in units of  $10^{-6} \text{ Mpc}^{-1}$ .

the WMAP team [11], which correctly accounts for correlations between values of  $\ell$  and the non-Gaussian shape of the distribution. For the fiducial model it is equal to 0.00094, which is the value that we will need when comparing to other models.

### III. LOW-POWER MODELS

#### A. A flat universe with a cutoff in the primordial spectrum

The most obvious way to lower the CMB power spectrum is to lower the power in the primordial density power spectrum  $P(k)$  [12–16]. Since the CMB is the product of small fluctuations in the primordial plasma, we can use linear theory. To each multipole  $\ell$  there corresponds a transfer function  $T_\ell(k)$ , such that  $\ell(\ell+1)C_\ell = 2\pi \int d \ln k T_\ell(k) k^3 P(k)$ . The transfer function depends on the cosmological parameters, but is peaked at approximately  $k \eta_0 \sim \ell$ , where  $\eta_0$  is the current size of the Universe, of order  $\eta_0 \sim 1.5 \times 10^4 \text{ Mpc}$ . Lowering power at  $k \leq 6 \times 10^{-4} \text{ Mpc}^{-1}$  thus lowers the CMB power spectrum for  $\ell \leq 4$ .

A simple model where such a cutoff was imposed by fiat was considered by Contaldi *et al.* [16]. They used the following form for the primordial spectrum:

$$P(k) = P_0(k) [1 - e^{-(k/k_c)^\alpha}], \quad (7)$$

where  $P_0(k) = A k^n$  is the usual power law primordial spectrum. They rightly determine that the data favor a cutoff at  $k_c \approx (5-6) \times 10^{-4} \text{ Mpc}^{-1}$ . In Ref. [16] Contaldi *et al.* considered another class of models with the cutoff produced by altering the shape of the inflaton potential. Here, we concentrate on the lower multipoles alone and consider the effect of varying *only* the location of the power cutoff using Eq. (7) with  $\alpha = 1.8$ . This reasonably assumes that there is enough freedom in the model space to allow the high- $\ell$  spectra to adjust to fit the data, and that the transfer function,  $T_\ell(k)$ , does not change much at low  $\ell$ .

In Fig. 3 we show the CMB power spectrum at low multipoles with several cutoff models, and in Fig. 4 we show the

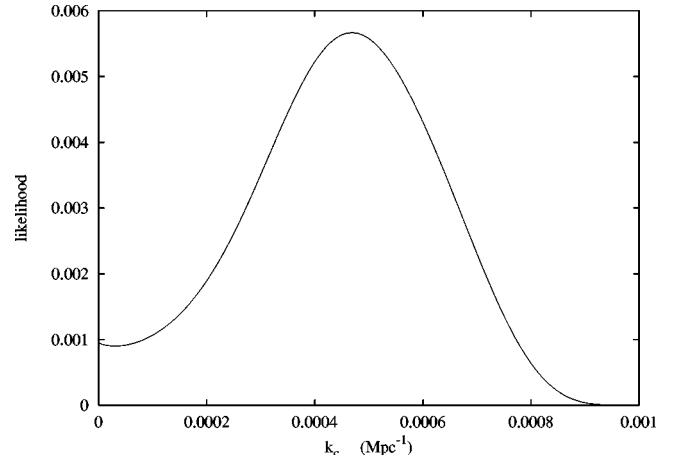


FIG. 4. The likelihood as a function of the cutoff wave number  $k_c$  for the model of Sec. III A.

CMB likelihood as a function of the cutoff scale,  $k_c$ . These figures essentially reproduce the results of Contaldi *et al.*

It is clear that the cutoff allows for a better fit than the so-called best fit. Next we evaluate the evidence for this model with  $k_c$  as the only parameter, with the prior  $p(k_c) \equiv P(k_c | \text{cutoff})$  chosen to be flat in the region  $[0, 0.001] \text{ Mpc}^{-1}$ . We obtain

$$P(D | \text{cutoff}) = \int dk_c p(k_c) \mathcal{L}(k_c) = 0.0025. \quad (8)$$

This value is 2.6 times the evidence for the fiducial model, which implies that the cutoff model is preferred only at the approximately  $1.4\sigma$  level. We have also calculated the Ockham factor for this model, defined in Eq. (5), to be 0.441.

Choosing a flat prior over this region emphasizes values of the cutoff near  $k_c \sim 0.5 \times 10^{-3} \text{ Mpc}^{-1}$ , so in fact implements a sort of fine tuning. We might instead use a prior proportional to  $1/k_c$  (i.e., linear in  $\ln k_c$ ), which also has the advantage of having the same form if we switch variables to the cutoff length  $l_c \propto 1/k_c$ . If we choose a lower limit of  $10^{-4} \text{ Mpc}^{-1}$ , the evidence is unchanged from the value for the flat prior, but as we decrease the lower limit the evidence becomes dominated by the plateau at  $k_c \rightarrow 0$ , where the models approach the fiducial best fit. The limiting value of the evidence is thus the same value as for the fiducial model itself: the maximum likelihood for this model may be quite large, but the Ockham factor is small.

#### B. Geometry: A closed universe

CMB measurements indicate that the geometry of the Universe is very nearly flat. This is consistent with the inflationary paradigm in which the Universe, unless additionally fine-tuned, would be expected to be infinitesimally close to flat today. However, a slightly closed universe is also consistent with the current data and is actually marginally preferred by the WMAP experiment [2], whose best-fit value was  $\Omega_k = -0.02 \pm 0.02$ .

When calculating theoretical predictions for CMB anisotropy spectra one is faced with the so-called geometric degen-

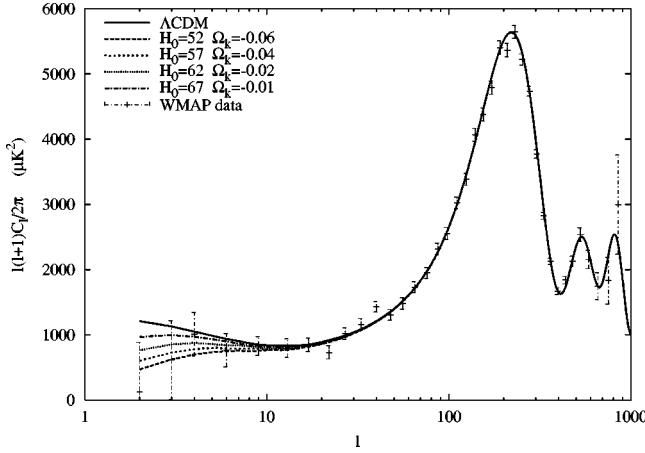


FIG. 5. The CMB power spectrum for different curvature values in the closed model of Sec. III B.

eracy among the values of matter density, curvature, and dark energy density [17]. Given fixed values for  $\Omega_{\text{CDM}}h^2$ ,  $\Omega_b h^2$ , and the acoustic peak location parameter one can produce almost identical CMB spectra by choosing the values of  $h$  and  $\Omega_k$  along a degeneracy line in the  $(h, \Omega_k)$  space. The differences between spectra are only notable on large scales ( $\ell \lesssim 20$ ) where the integrated Sachs-Wolfe contribution to the anisotropy due to the dark energy component is dominant.

A closed universe contains a characteristic scale—the curvature scale  $R_c$ . The eigenvalues  $\beta$  of the Laplacian are, therefore, discrete and related to the physical wave number  $k$  via  $\beta^2 = 1 + k^2 R^2$  with modes corresponding to  $\beta = 1$  and 2 being unphysical pure gauge modes. As argued in Ref. [18], if the Universe was indeed marginally closed, in the absence of a concrete model it is not obvious how the concept of scale invariance should be extended to scales comparable to the curvature scale. One of the possibilities could be that the spectrum would truncate on scales close to  $R$ . A heuristic formula for the primordial spectrum, illustrating such a possibility, was suggested in Ref. [18]:

$$P(\beta) \propto \frac{(\beta^2 - 4)^2}{\beta(\beta^2 - 1)} \left[ 1 - \exp\left(-\frac{\beta - 3}{4}\right) \right]. \quad (9)$$

We have used Eq. (9) to generate CMB anisotropy spectra for various values of  $\Omega_k$  chosen to lie along the same geometrical degeneracy line that contained WMAP's best-fit  $\Lambda$ CDM model. The results are shown in Fig. 5. As can be seen from the plot, the truncated closed models fit the data considerably better than WMAP's best-fit model. We show the likelihood as a function of the Hubble constant in Fig. 6.

Next we calculate the evidence for this model with  $h$  as the free parameter. The prior  $p(h)$  was taken to be a Gaussian with mean  $\bar{h} = 0.72$  and variance  $\sigma_h = 0.10$ , and additionally constrained to be in the range  $[0.52, 0.72]$ . The lower bound is dictated by current experimental constraints on the value of  $h$ , while the upper bound follows from the fact that along the geometric degeneracy line higher values of  $h$  would correspond to  $\Omega_k \geq 0$ . We find that the evidence for this model is

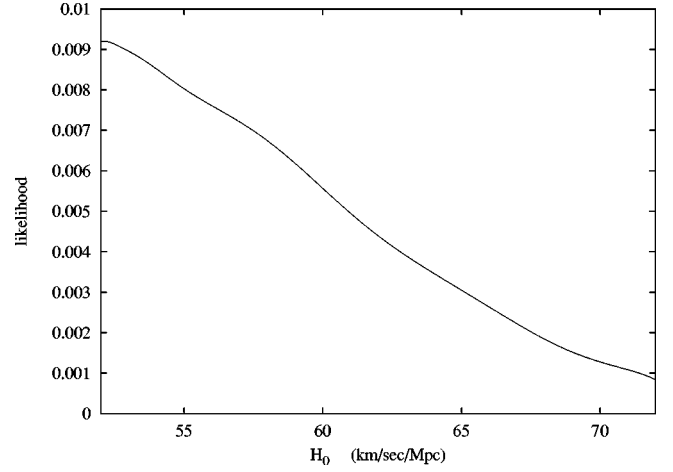


FIG. 6. The likelihood as a function of  $H_0$  for the closed model of Sec. III B.

$$P(D|\text{closed}) = \int dh p(h) \mathcal{L}(h) = 0.0034, \quad (10)$$

where  $\mathcal{L}(h)$  is the likelihood of data given a particular value of  $h$ . The obtained evidence is approximately 3.6 times that of WMAP's best-fit model. This can be interpreted as the closed model being preferred over the best-fit model at a  $1.6\sigma$  level, which, considering the absence of a robust model of a marginally closed universe, is insufficient to warrant abandoning simple inflation as the base model for fitting data. The Ockham factor for this model [Eq. (5)] is 0.370.

In addition, we have considered the same closed universe model but with the spectral index  $n_s$  and also the value of  $\sigma_8$  allowed to vary to see if the fit could be improved further. The prior on  $n_s$  was chosen to be Gaussian with  $\bar{n} = 0.97$  and  $\sigma_n = 0.07$  and restricted to the interval  $[0.83, 1.11]$ . The prior on  $\sigma_8$  was also Gaussian with the mean value of 0.95 and variance 0.05 restricted to the range  $[0.6, 1]$ . We found the evidence in this case to be

$$P(D|\text{closed}) = \int dn dh d\sigma_8 p(n) p(h) p(\sigma_8) \mathcal{L}(n, h, \sigma_8) = 0.0008, \quad (11)$$

which is lower than the evidence for the fiducial model. The likelihood contours for this model, after marginalizing over  $\sigma_8$ , are shown in Fig. 7. This illustrates how adding more parameter freedom can dramatically dilute the evidence for the model, even if it fits the data very well. This is reflected in a very low value of the Ockham factor for this model, which is only 0.069.

#### IV. THEORETICAL AND EXPERIMENTAL SYSTEMATICS

Having examined the possibility that the observed lack of power on large scales points in the direction of new physics, we now turn to the alternative that it can be attributed to data analysis methodology. The simplest case would be an under-



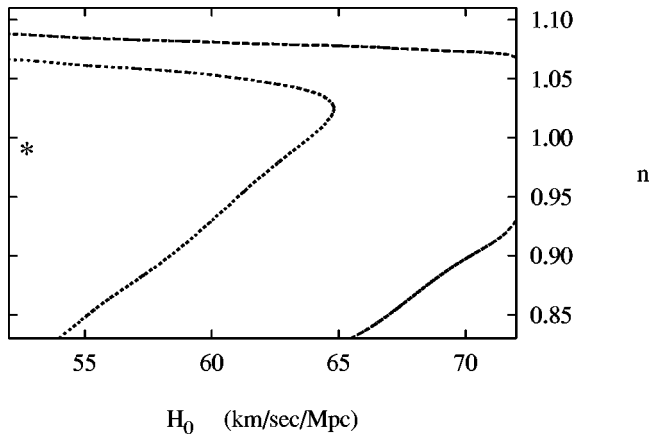


FIG. 7. Likelihood contours in the  $(n, h)$  parameter space for the closed model of Sec. III B, marginalized over the value of  $\sigma_8$ . Shown are the  $1$  and  $2\sigma$  contours, defined by the equivalent likelihood ratio for a two-parameter Gaussian distribution. The point that maximizes the likelihood function is marked with an asterisk (\*).

estimation of the errors corresponding to low multipoles. This would mean that we live in a universe described by the best-fit power-law model and that the discrepancy between its predictions and the WMAP data emanates from our miscalculating the aforementioned errors. Of course, we have copious evidence from the work done by the WMAP team itself as well as from comparison with other data that the WMAP data are likely to be reliable on these scales. Conversely, we could instead interpret this as saying that the  $\ell = 2, 3$  multipoles are correctly measured, but have an unknown origin outside the standard cosmology. That is, there is some model like those considered in the previous sections, but we do not yet know what it is.

We implement this idea by multiplying the diagonal elements of the curvature matrix corresponding to  $C_2$  and  $C_3$  by two constants (hereafter referred to as  $r_2$  and  $r_3$ ) that serve as the free parameters of our model. This has the effect of increasing the error bars of  $C_2$  and  $C_3$ . Figure 8 shows contours of the likelihood function for various values of these

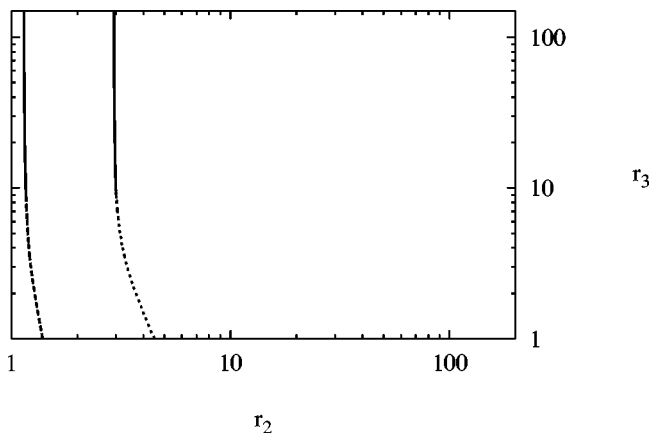


FIG. 8. Contours of the likelihood as a function of the parameters  $r_2$  and  $r_3$ . Shown are the  $1$  and  $2\sigma$  contours. The likelihood is maximized in the upper right corner, where  $r_2$  and  $r_3$  are largest.

TABLE I. Summary of the results of the paper. The Bayes factors,  $B$ , are all defined with respect to the “best fit” model of the first row, and the column “ $\sigma$ ” is defined as  $\sqrt{2|\ln B|}$ . The Ockham factors are defined in the text, Sec. I.

Model	Ockham factor	Bayes factor	$\sigma$
Best fit	-	1	-
Flat with cutoff	0.441	2.66	1.40 $\sigma$
Closed ( $h$ )	0.370	3.62	1.60 $\sigma$
Closed ( $h \sigma_8 n$ )	0.069	0.85	0.57 $\sigma$
Large error bars	0.945	41.2	2.73 $\sigma$

parameters. We have also evaluated the evidence for this model to be

$$P(D|\text{syst.}) = \int dr_2 dr_3 p(r_2) p(r_3) \mathcal{L}(r_2, r_3) = 0.0387, \quad (12)$$

using flat priors on  $r_2$  and  $r_3$  in the intervals  $[1, 200]$  and  $[1, 150]$  respectively; these maxima are chosen for numerical convenience but the results are insensitive to them as long as  $r_i \gg 1$ . It is also insensitive to whether we use a uniform prior on the  $r_i$  or on  $\ln r_i$ . The latter are equivalent to  $P(r_i) \propto 1/r_i$ , the so-called “Jeffreys’ prior” appropriate for a scale parameter.

Note that the likelihood is maximized when these parameters reach their largest values: the data always become more likely when the error bars increase. Indeed, this implies that we can consider an even simpler model with parameters fixed at  $r_i \rightarrow \infty$ . This model has a likelihood of 0.0414, giving it a Bayes factor of 44 with respect to the conventional best fit. This model corresponds to ignoring the data at  $\ell = 2, 3$ : there is *no model* that can improve the fit here by more than this roughly  $2.75\sigma$  level. The evidence for these models implies that if the correct model at low  $\ell$  was indeed other than the “best fit,” there would be a roughly  $2.75\sigma$  level evidence that the error bars on  $C_2$  and  $C_3$  were underestimated.

## V. DISCUSSION

We summarize our results in Table I, presenting the Bayes and Ockham factors for the models we have discussed. Note that these numbers explicitly do not consider prior information about these models. Indeed, all of these models were explicitly constructed in response to the observed low power. In particular, the models with low primordial power considered in Sec. III require that the scale of the power cutoff be fine tuned with respect to the horizon scale in order to reduce power at just the right angular scale, either by fiat or by determining the location of the curvature scale. *A priori*, such models would be strongly disfavored. However, it has been recently pointed out in Ref. [19] that a cross-correlation between CMB and cosmic-shear patterns, as well as between CMB and low-redshift tracers of the mass distribution, can provide supplemental evidence for a large scale cutoff in the primordial spectrum. Such a cutoff would generally increase the cross-correlation.

There are models with similar characteristics that have been discussed separately from these low-power issues: the class of models with nontrivial topologies [20–26]. We might assign a greater prior to such models, although again to explain the observations requires fine tuning of the topology scale. In a recent paper Tegmark *et al.* [27] argued that the low power on large scales is unlikely to be a sign of nontrivial topology. We did not include these models into our analysis; however, one can expect them to have evidence similar to the cutoff models we have considered. Indeed, the type of CMB spectra that these two models produced are essentially the same and the difference in the values of the evidence comes mainly from the prior on the free parameter. Note that models with nontrivial topology will also have other signatures, possibly observable in the CMB by considering properties beyond the power spectrum (see e.g., Ref. [25] and references therein).

Other analyses of these data have reached similar conclusions. In Ref. [28] Gaztañaga *et al.* performed a full covariance analysis of the WMAP data using the two-point angular correlation and its higher-order moments. They have argued that the WMAP data are in reasonable agreement with the  $\Lambda$ CDM model if WMAP data were considered as a particular realization of realistic  $\Lambda$ CDM simulations with the corresponding covariance.

We have also considered a model that considers a possible systematic error in the determination of the large-scale power. Although this model is experimentally unlikely, we can instead consider it as the *reductio ad absurdum* of all the possibilities we are considering: What happens if we just

throw away the large scale data? From the Bayes factor of about 44 we see that there is likely *no model* at all that will ever improve the fit to the large scale by more than about  $2.75\sigma$ , in agreement with the somewhat different analysis of Ref. [29] and to some extent with that of the WMAP team itself [1,2]. It is worth noting that the phases of low harmonics could provide additional information about the plausibility of a cosmological model; for instance, a model predicting an alignment of the  $\ell=2,3$  harmonics (according to Ref. [26]) would be favored with respect to a model making no such prediction, given that both models had the same power at low  $\ell$ . But we should point out that features like the alignment of the low harmonics would not have any impact on the power at large scales. Consequently, no model will ever fare better than about  $2.75\sigma$  as far as power at large scales is concerned.

However, there are other possibilities for probing the physics on the largest scales. In particular, a better measurement of the polarization of the CMB and its correlation with the intensity at these same multipoles will certainly enable us to clarify the interpretation of the anisotropy at the same scales.

# ACKNOWLEDGMENTS

A.H.J. would like to thank G. Efstathiou for helpful conversations. A.H.J. and L.P. were supported by PPARC in the UK, and A.N. by EC network HPRN-CT-2000-00124, “CMBnet.”

- 
- [1] C.L. Bennett *et al.*, *Astrophys. J., Suppl. Ser.* **148**, 1 (2003).
  - [2] D.N. Spergel *et al.*, *Astrophys. J., Suppl. Ser.* **48**, 175 (2003).
  - [3] E. T. Jaynes, *Probability Theory: The Logic of Science* (Cambridge University Press, Cambridge, UK, 2003).
  - [4] T.J. Loredo, in *Maximum-Entropy and Bayesian Methods, Dartmouth, 1989*, edited by P. Fougere (Kluwer Academic, Dordrecht, 1990), pp. 81–142.
  - [5] A. Jaffe, *Astrophys. J.* **471**, 24 (1996).
  - [6] M.P. Hobson, S.L. Bridle, and O. Lahav, *Mon. Not. R. Astron. Soc.* **335**, 377 (2002).
  - [7] T.D. Saini, J. Weller, and S.L. Bridle, *astro-ph/0305526*.
  - [8] M.V. John and J.V. Narlikar, *Phys. Rev. D* **65**, 043506 (2002).
  - [9] P.S. Drell, T.J. Loredo, and I. Wasserman, *Astrophys. J.* **530**, 593 (2000).
  - [10] M. Zaldarriaga and U. Seljak, URL <http://www.cmbfast.org/>.
  - [11] H.V. Peiris *et al.*, *Astrophys. J., Suppl. Ser.* **148**, 213 (2003).
  - [12] J. Yokoyama, *Phys. Rev. D* **59**, 107303 (1999).
  - [13] S.L. Bridle, A.M. Lewis, J. Weller, and G. Efstathiou, *Mon. Not. R. Astron. Soc.* **342**, L72 (2003).
  - [14] J.M. Cline, P. Crotty, and J. Lesgourgues, *J. Cosmol. Astropart. Phys.* **09**, 010 (2003).
  - [15] B. Feng and X. Zhang, *Phys. Lett. B* **570**, 145 (2003).
  - [16] C.R. Contaldi, M. Peloso, L. Kofman, and A. Linde, *J. Cosmol. Astropart. Phys.* **7**, 2 (2003).
  - [17] G. Efstathiou and J.R. Bond, *Mon. Not. R. Astron. Soc.* **304**, 75 (1999).
  - [18] G. Efstathiou, *Mon. Not. R. Astron. Soc.* **343**, L95 (2003).
  - [19] M.H. Kesden, M. Kamionkowski, and A. Cooray, *Phys. Rev. Lett.* **91**, 221302 (2003).
  - [20] I.Y. Sokolov, *Pisma Zh. Éksp. Teor. Fiz.* **57**, 601 (1993) [*JETP Lett.* **57**, 617 (1993)].
  - [21] D. Stevens, D. Scott, and J. Silk, *Phys. Rev. Lett.* **71**, 20 (1993).
  - [22] Y. Jing and L. Fang, *Phys. Rev. Lett.* **73**, 1882 (1994).
  - [23] A. de Oliveira-Costa and G.F. Smoot, *Astrophys. J.* **448**, 477 (1995).
  - [24] G. Rocha *et al.*, *astro-ph/0205155*.
  - [25] J. Levin, *Phys. Rep.* **365**, 251 (2002).
  - [26] A. de Oliveira-Costa, M. Tegmark, M. Zaldarriaga, and A. Hamilton, *Phys. Rev. D* (to be published), *astro-ph/0307282*.
  - [27] M. Tegmark, A. de Oliveira-Costa, and A. Hamilton, *Phys. Rev. D* **68**, 123523 (2003).
  - [28] E. Gaztanaga, J. Wagg, T. Multamaki, A. Montana, and D.H. Hughes, *Mon. Not. R. Astron. Soc.* **346**, 47 (2003).
  - [29] G. Efstathiou, *Mon. Not. R. Astron. Soc.* **346**, L26 (2003).